

***Saccharomyces cerevisiae* microfiltration performance of polycarbonate membranes containing chitosan-based polyelectrolyte complexes**

Rayane S. Vale, Caio M. Paranhos 

Polymer Laboratory, Department of Chemistry, Federal University of São Carlos, Via Washington Luís km 235, São Carlos, São Paulo 13565-905, Brazil

Correspondence to: C. M. Paranhos (E-mail: paranhos@ufscar.br)

ABSTRACT: Polyelectrolyte complexes (PECs) were prepared using chitosan and sulfonated poly(ethylene terephthalate) by the mixture method. Fourier transform infrared spectroscopy, zeta potential, X-ray diffraction, and thermogravimetric analysis were used to characterize the chemical structure, surface charge, crystallinity, and thermal stability of the PECs. To evaluate how PECs affect the water vapor flux and the microfiltration performance, PECs solutions were spread via casting on polycarbonate microporous membranes. The increase in water vapor flux and in the *Saccharomyces cerevisiae* microfiltration performance indicated that the presence of the PECs acts as fixed charges, changing significantly the transport properties of the polycarbonate matrix. © 2019 Wiley Periodicals, Inc. *J. Appl. Polym. Sci.* 2019, 136, 48483.

KEYWORDS: microfiltration; polyelectrolyte complexes; polymer membrane; *Saccharomyces cerevisiae*; transport properties

Received 20 February 2019; accepted 20 August 2019

DOI: 10.1002/app.48483

INTRODUCTION

Polyelectrolyte complexes (PECs) are spontaneously formed through electrostatic interactions when polyelectrolytes (PELs) with opposite charges are mixed.¹ PECs can be used in drug delivery systems,^{2,3} to improve papermaking properties,⁴ for mechanical strengthening of cotton fibers,⁵ for flocculation,⁶ in tissue engineering,⁷ and in separation membranes.^{8,9}

Surface modification can change hydrophilicity, selectivity, and permeability and reduce fouling in polymeric membranes.¹⁰ A great number of modification strategies have been employed for this purpose, as the use of specific additives,¹¹ coating,¹² interfacial polymerization,¹³ plasma treatment,¹⁴ graft polymerization,¹⁵ incidence of high energy particles,¹⁶ heat treatment,¹⁷ and chemical reactions as carboxylation, sulfonation, amination, and epoxidation.¹⁸ Some physical properties of the PECs, as chemical stability, hydrophilicity, and tunable surface charges, also make them interesting materials to modify the surface of polymer membranes.¹⁹ From this point of view, modification of membranes with PECs based on polymers from renewable sources with low cost and low-complexity methodology is still few investigated.²⁰

Chitosan (CH) (Figure 1) is one of the most used polycations to prepare PECs.²¹ CH is derived from the deacetylation of chitin. Therefore, it has an almost unlimited source of raw material because some of the large sources of chitin are shells of crustaceans, fungal cell

walls, and exoskeleton of insects.²² Other reason for the great interest in CH is due to some of its characteristics as biocompatibility, hydrophilicity, biodegradability, antibacterial properties, and bioactivity.²³

CH can form PECs with polyanions of different categories,²⁴ including synthetic polymers,²¹ metal anions,²⁵ and natural polymers.²⁶ The polyanion chosen for this investigation was sulfonated poly(ethylene terephthalate) (SPET), a synthetic copolymer with a structure similar to that of poly(ethylene terephthalate) (PET), except for the dimethyl isophthalate sodium sulfonate comonomer (Figure 2). Our research group have investigated the use of SPET in PEC-based hydrogels²⁷ and semi-interpenetrating (s-IPN) networks hydrogels.²⁸ This copolymer was chosen because of its well-known structure and due to its good solubility in water and high hydrophilicity.

In this study, PECs based on CH and SPET were synthesized by the mixing method, characterized, and deposited by casting on a microporous polycarbonate (PC) membrane. We focused the present investigation on the water transport properties and microfiltration of *Saccharomyces cerevisiae*. *Saccharomyces cerevisiae* is widely employed as yeast in different industrial segments as winery, brewing, and baking. Consequently, this yeast was chosen as model for microfiltration evaluation in order to observe how the structure-transport properties aspects of the PC membrane were modified by the PECs.

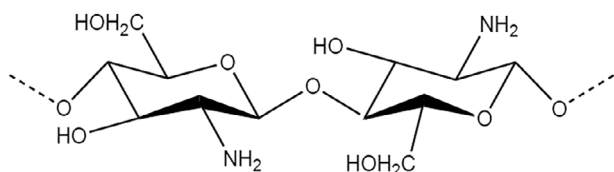


Figure 1. Chemical structure of chitosan.

EXPERIMENTAL

Reagents

Chitin was obtained from white leg shrimps (*Litopenaeus vannamei*) collected in Baia de Sepetiba, Rio de Janeiro (Brazil). CH was obtained by deacetylation of chitin, as described by Rege and Block.²⁹ The deacetylation degree of the obtained CH was 79% (determined by ¹H NMR) and $\overline{M}_v \sim 450,000 \text{ g mol}^{-1}$. SPET (13% per monomeric unit, $\overline{M}_n = 56,000 \text{ g mol}^{-1}$) was used as received from Solvay (Belgium). 5 μm PC membranes Isopore were purchased from Millipore. *S. accharomyces cerevisiae* was obtained by Fleishman (Brazil). The yeast culture was prepared in distilled water (1 g L^{-1}) at 30 °C.

Synthesis of CH-SPET PECs by the Dropping Method

The average molar mass of CH used in this investigation is about nine times greater than SPET. Also, the number of ionizable groups in CH is higher than SPET. For this reason, the CH content in PECs was kept constant, varying only the SPET content. The PEL solutions were prepared in an acid buffer solution (0.018 mol L^{-1} of sodium acetate, 0.082 mol L^{-1} of acetic acid, and 0.14 mol L^{-1} of NaCl). It was prepared a 1 g L^{-1} solution of CH and 1, 2 and 3 g L^{-1} solution of SPET. CH-SPET solutions were prepared by mixing negatively charged SPET solutions and positively charged CH solutions by the dropping method: 14 mL of a specified concentration of SPET was added dropwise into a 14 mL of CH solution under stirring in a high-speed homogenizer at 7000 rpm for 2 min. The sample nomenclature of the PECs was based on the proportion of the PELs (Table I).

Preparation of the PEC Modified Membranes

1 mL of the PEC solution was spread on the PC membranes with a doctor blade using a gap thickness of 40 μm . The membranes were dried in an oven at 80 °C for 3 h. The modified membranes were then kept immersed in distilled water at room temperature for 72 h to guarantee the release of soluble, unbounded PECs. Finally, the membranes were dried as described previously.

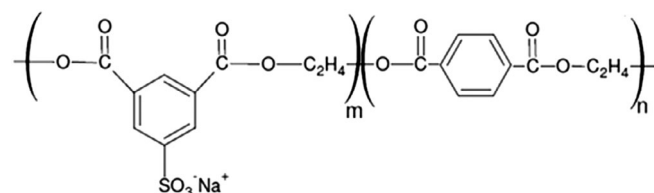


Figure 2. Chemical structure of SPET.

Table I. Nomenclature of the PECs and Concentration of the PELs

Sample	SPET concentration (g L^{-1})	CH concentration (g L^{-1})
PEC 1:1	1	
PEC 1:2	2	1
PEC 1:3	3	

Characterizations

Infrared spectra were collected in a Varian 640 FTIR spectrometer and recorded with 32 scans with a resolution of 4 cm^{-1} . The PECs were mixed with KBr and pressed for measurement. The zeta potential was quantified by Zeta Potential Analyzer (Brookhaven Instruments Corporation, Holtsville, NY). It was made 10 measurements for each sample. X-ray diffraction data were collected in a Rigaku DMax 2500PC diffractometer using Cu K α radiation ($\lambda = 1.5418 \text{ \AA}$) at room temperature and a scan rate of 2° min^{-1} . The samples were compressed in the sample holder without any adhesive substances. Thermogravimetric analysis (TGA) was conducted on a Netzsch 209 F3 Tarsus at a scanning rate of $20 \text{ }^\circ\text{C min}^{-1}$ from 40° to 600° C under a nitrogen atmosphere. The PECs and PECs membranes were examined by a field emission SEM (FEI INSPECT F-50). The samples were coated with a thin layer of gold by ions pattering prior to microscopic examination. The ImageJ software was used to calculate the average size of the obtained PECs.

Transport Properties

The water vapor flux (WVF) through the membranes was measured using the Payne cup technique (ASTM E96, at 30 °C). The system containing the Payne cup, water and the membrane was weighed, put into a desiccator and weighed at every hour, during 12 h. Water vapor transport was calculated according to eq. (1).

$$\text{WVF} = \frac{\Delta m}{\Delta t} \frac{1}{A} \quad (1)$$

where WVF is the water vapor flux, Δm is the mass difference, Δt is the time difference, and A is the membrane area.

The membrane potential measurements were performed in diaphragm-type cell, made up of polyamide 6. The cell is based in two chambers separated by the membrane (effective area 4.0 cm^2). The same cell was used to determine the cation transport number (t_+). Two solutions of different concentrations were added on each side of the cell, so that the ratio (r) between the two concentrations was $r = \text{CI}/\text{CII} = 10$. To measure the potential, a Minipa ET-2231A multimeter was used. The reference electrodes used, reversible to the chloride anion, were of saturated calomel. The experiment was performed with 0.1 M and 1.0 M potassium chloride solutions. Voltage values were collected every approximately 10 min for a period of approximately 4 h at 25 °C. The membrane potential is related to t_+ by the following equation³⁰:

$$E_m = 2t_+ \frac{RT}{F} \ln \frac{a_2}{a_1} \quad (2)$$

where E_m is the membrane potential, R is the gas constant, F is the Faraday constant, and a is the ion activity in chambers 1 and 2.

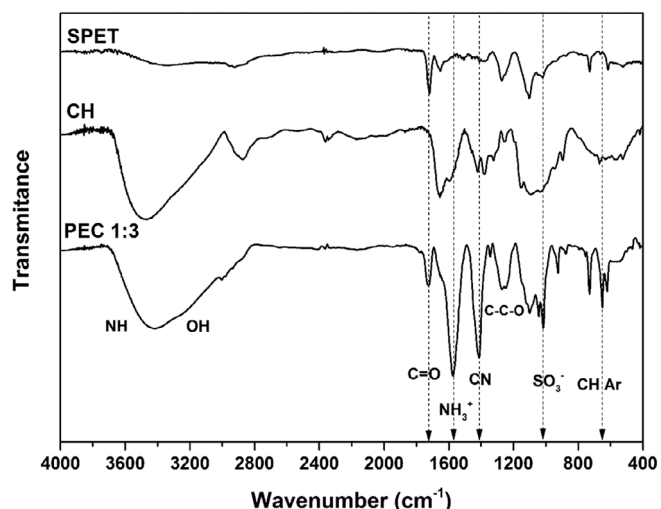


Figure 3. FTIR spectra of SPET, CH, and PEC 1:3.

Saccharomyces cerevisiae Microfiltration

Microfiltration performance of the membranes was evaluated in a dead-end module Stirred Cell 8050 (Millipore Corporation), under filtration pressure of 1.5 bar (N_2). The number of microorganisms in 0.1 μ L of the filtrated solutions were counted using a Neubauer chamber mounted in an Olympus Bx50 microscope, with integrated digital camera Olympus DP72.4.1.

RESULTS AND DISCUSSION

Characterization of the PECs and Membranes

The infrared absorption spectrum of CH, SPET, and PEC 1:3 is shown in Figure 3. The bands were attributed according to the literature. The presence of the typical bands of CH: 1661–1671 cm^{-1} , axial deformation of C=O amide I; 1583–594 cm^{-1} , angular deformation of N–H; 1380 and 1383 cm^{-1} , symmetric angular deformation of CH_3 ; 1308 and 1380 cm^{-1} , axial deformation of CN of amino groups^{31,32} are confirmed. In the spectrum of SPET, a carbonyl group in conjugation with an aromatic ring is observed at 1719 cm^{-1} and a signal of C=C in aromatics at 1506 cm^{-1} . The band at 1272 cm^{-1} is due to the asymmetric C–C–O stretch involving the carbon of an aromatic group. There is an asymmetric O–C–C stretch at 1104 cm^{-1} and a subtle band at 1046 cm^{-1} , characteristic of the symmetrical vibrations of the SO_3^- group. The signal at 730 cm^{-1} corresponds to the stretching of the C–H bond of aromatics.³³

The spectrum of the three PECs was all similar, so that the PEC 1:3 was chosen to represent the PECs. The spectrum showed the appearance of a new band corresponding to the $-NH_3^+$ group in the 1570 cm^{-1} region.³⁴ At about 1040 cm^{-1} , the PECs present

Table II. Zeta Potential of the PELs and PECs

PEL	ZP (mV)	PEC	ZP (mV)
CH (1 g L ⁻¹)	23 ± 2	PEC 1:1	40 ± 3
SPET (1 g L ⁻¹)	-45 ± 8	PEC 1:2	35 ± 3
SPET (2 g L ⁻¹)	-54 ± 3	PEC 1:3	28 ± 4
SPET (3 g L ⁻¹)	-59 ± 5		

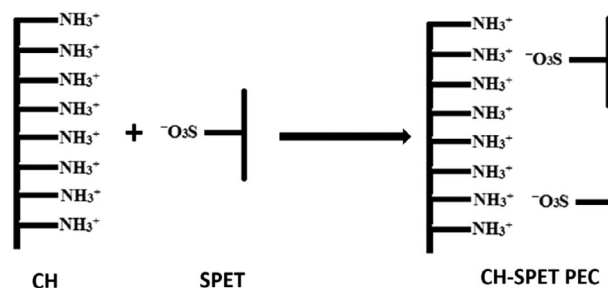


Figure 4. CH-SPET PEC formation scheme.

the characteristic band of the $-SO_3^-$ group. These FTIR results are indicative of the existence of the complexation reaction between the $-SO_3^-$ groups and the protonated amine groups of chitosan by electrostatic interactions, resulting in the PECs.

Table II shows the zeta potential of PELs and PECs. SPET is a strong PEL, so it is fully charged in solution and presented negative values of ZP. As for CH, it has most of the amino groups protonated in pH lower than 6.5. The pH of the solutions in this work was 3.6, so CH showed positive values of ZP. When the CH solution is dropped into SPET solution, intermolecular electrostatic attractions occurred between the anionic groups from SPET and cationic amino groups of CH and a PEC is formed (Figure 4).

The zeta potential of PECs, listed in Table II, showed that they have charges of about 28–40 mV. These values are due to the difference between the degree of ionization of the PELs. The CH sample has 79% of amino groups, SPET sample, although, has only 13% of sulfonate groups. So, the PECs show positive values of zeta potential. As the SPET concentration increases, more positive groups are neutralized and the zeta potential of the PECs decreases. Therefore, tunable surface charges can be easily obtained by CH:SPET composition.

Figure 5 presents the XRD patterns of the PELs and PECs. The SPET has characteristic diffraction of amorphous substances, whereas the CH presents crystalline domains in its

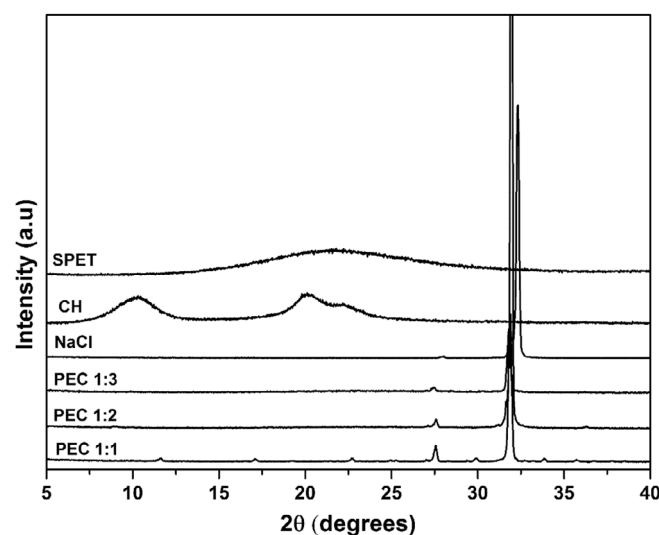


Figure 5. XRD patterns of SPET, CH, and PECs.

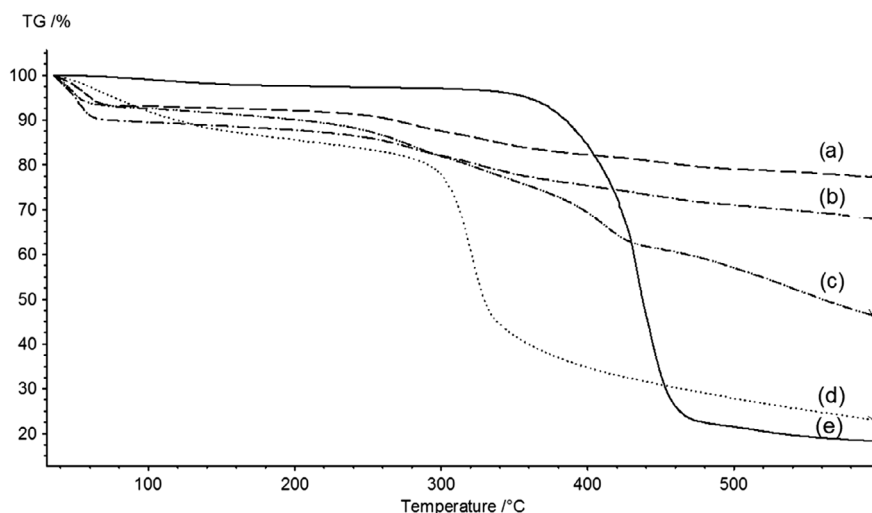


Figure 6. TGA curves of PEC 1:1 (a), PEC 1:2 (b), PEC 1:3 (c), CH (d), and SPET (e).

structure (peaks in the region of 2θ between 11° and 20°). This crystallinity is a result of hydrogen bonds between the CH chains.³⁵

The PECs were made in solutions containing NaCl. Therefore, the X-ray diffraction of this salt was obtained. This measure proved to be prudent because the characteristic NaCl signals appeared in all PEC diffractions. The diffraction patterns of the PECs indicate that these are amorphous. This characteristic is justified by the loss of the crystalline domains of CH, because the electrostatic interactions in the PECs are more intense than the hydrogen bonds between the CH chains.³⁶

The TGA curves and the first derivative of the thermal decomposition (DTGA) of CH and SPET are shown in Figure 6 and 7, respectively. The TGA curves of both PELs show one stage of intense mass loss. This stage is attributed to the degradation of the PELs. The temperature at which the degradation process becomes irreversible was obtained by the onset method and was 305°C for the CH and 384°C for the SPET. This behavior shows that the SPET is more thermally stable than CH. The thermal

behavior of the pure PECs presented higher thermal stability than the PELs, as can be observed by the greater residual mass of the complexes and their low mass variation throughout the heating process. This occurs because of the strong electrostatic interactions between the PELs. DTGA curve of PEC 1:1 and PEC 1:2 shows two peaks in the region between 200°C and 400°C , the first at around 280°C and the second at around 325°C . In the PECs, there are segments of CH, which do not interact with the SPET and therefore behave as pure CH. These regions presented degradation temperature around 325°C , close to the degradation temperature observed to the pure CH. Consequently, the peak at 278°C is probably related to segments of the CH that interact with the SPET. This behavior was also observed to PEC 1:3. However, a new peak can be observed at 409.5°C for PEC 1:3. This peak is intermediate between polycation and polyanion maximum degradation temperature. Therefore, this peak can be attributed to the higher content of SPET interacting with CH cationic groups. These interactions alter simultaneously the thermal resistance of SPET and CH, resulting in this new peak.

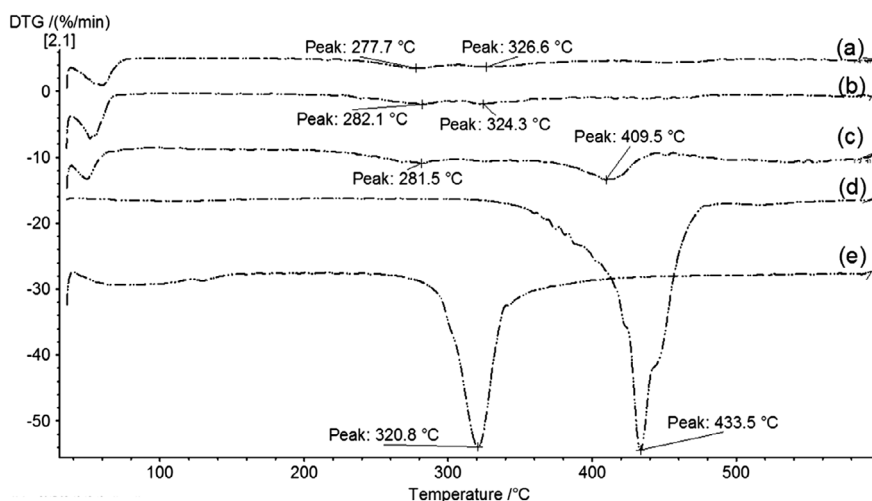


Figure 7. DTGA curves of (a) PEC 1:1, (b) PEC 1:2, (c) PEC 1:3, (d) SPET, and (e) CH.

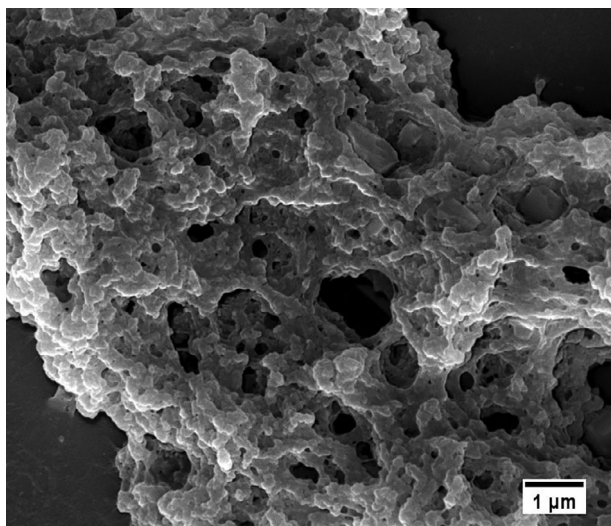


Figure 8. SEM micrograph of PEC 1:1.

The micrograph of PEC 1:1 is shown in Figure 8 and the other PECs have a very similar morphology. It is possible to note that the PECs are formed of aggregate particles, what agrees with the literature.¹⁹ SEM also confirmed the stable deposition of the PEC onto the PC membrane. Figure 9(a) shows the PC membrane, which has homogeneous porous and no component deposited on its surface. On the other hand, it is possible to see the PEC 1:3 on the surface of PC membranes [Figure 9(b)]. The PECs have different sizes and are not well distributed on the membrane

what can be due to the method used to spread the PEC. The average size of the PEC 1:3 was $0.35 \pm 0.19 \mu\text{m}$. It was also noted that some PECs cover the pores of the membranes and therefore must be observed within them, as shown in Figure 9(c). It is possible to note that the localization of the PECs is random due to the casting method adopted.

Water Vapor Flux

WVF was measured to evaluate the change in the water affinity caused by the PECs in the PC membranes. Table III shows the values obtained for WVF. The high standard deviation values of some samples and the large difference between the variations can be related to the inhomogeneity of the PECs onto the surface of the membranes. A previous study of our research group showed that a dense PC matrix presents a WVF in the order $4 \text{ g day}^{-1} \text{ m}^{-2}$,³⁷ which demonstrates that PC has low affinity to water. In this work, the PC membrane presented pores of $5 \mu\text{m}$, which justifies its high WVF ($1019 \pm 4 \text{ g day}^{-1} \text{ m}^{-2}$).

However, it is possible to observe that the modified membranes showed a significant increase in WVF when compared to the PC control. As shown in Figure 9(c), the unmodified membrane has its pores unobstructed and the modified one presents clusters of PECs clogging the pores. It seems that these clogs increase the hydrophilicity of the pores and consequently the flux of water vapor when compared to the PC control. The water vapor molecules that pass through the clogged pores can solvate the PECs. Consequently, the presence of the PECs into the pores increases the local water affinity and, therefore, the WVF when compared to unmodified PC membrane. However, it is possible to note that

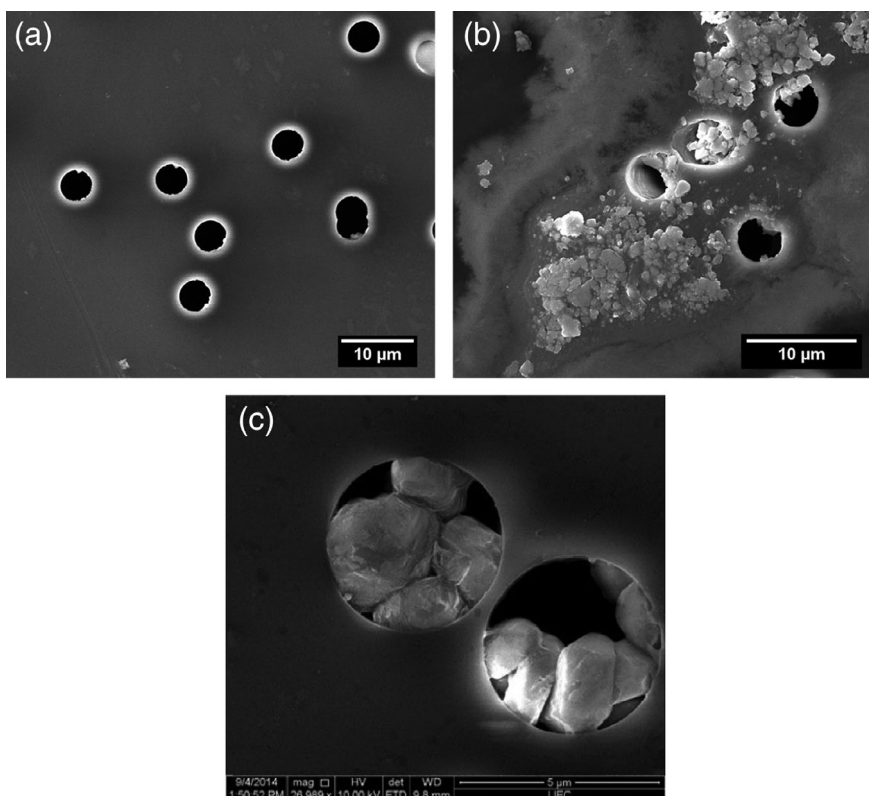


Figure 9. SEM micrograph of (a) PC membrane, (b) PC membrane with PEC 1:3, and (c) details of pores containing PECs.

Table III. WVF for the PC and Modified Membranes

Membrane	WVF ($\text{g}\cdot\text{day}^{-1}\cdot\text{m}^{-2}$)
PC	1019 ± 4
PEC 1:1	1523 ± 1
PEC 1:2	1798 ± 249
PEC 1:3	2070 ± 85

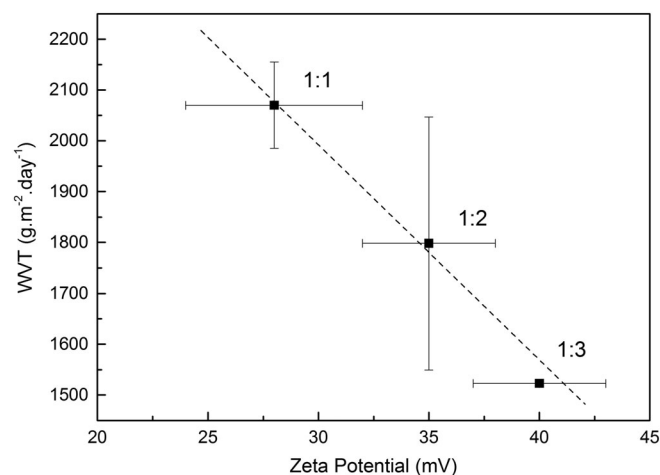
the SPET content into the PECs influences WVF. Since the average sizes of the obtained PECs are similar ($0.35 \pm 0.19 \mu\text{m}$), it seems that the pores are clogged in the same tendency. To clarify this aspect, Figure 10 shows the relationship between WVF and zeta potential of PECs.

It is possible to note in Figure 10 that higher the SPET content lower the zeta potential and WVF.

As the concentration of SPET increases in PECs, the number of cationic groups in CH, which are neutralized by the polyanion increases, diminishing the zeta potential. This result indicates that the SPET presents higher water affinity than CH and plays an important role on the control of WVT.

Microfiltration of *Saccharomyces cerevisiae*

Modified and unmodified membranes were used to filtrate a yeast solution to observe how the microfiltration of the PC membrane was modified by the PECs. To compare the performance of the membranes, the organisms in the filtered solution were counted using an optical microscope and a Neubauer chamber. PECs were not observed in the visual field of the Neubauer chamber indicating the fixation of the PECs onto the membrane even after microfiltration. Table IV shows the mean number of organisms in 0.1 μL of the filtered solutions. The membranes with PECs retain a larger number of microorganisms than the PC membrane, which retained 72%. There are two reasons for this behavior: the first one is the presence of clusters of PECs into the pores of the modified membranes [Figure 9(c)], which can clog the pores and be an

**Figure 10.** Relationship between WVF and zeta potential of the obtained membranes containing PECs. Dotted line used as visual reference.**Table IV.** Average Number of Organisms *Saccharomyces cerevisiae* Present in 0.1 μL of the Yeast Solution and the Filtrates for the PC and Modified Membrane

Samples	Average number of organisms
<i>Saccharomyces cerevisiae</i>	65.25
PC	18.00
PEC 1:1	7.25
PEC 1:2	0.75
PEC 1:3	3.25

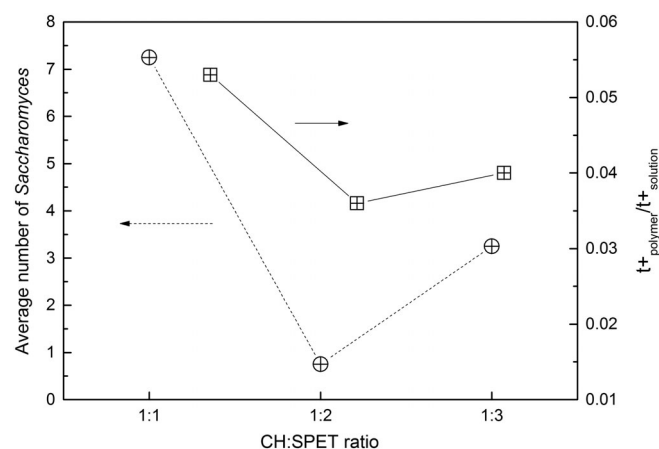
Table V. Membrane Potential and Transport Number of PC Membranes Modified With PECs

Membrane	Membrane potential (mV)	$t^+_{\text{polymer}}/t^+_{\text{solution}}$
PEC 1:1	2.74 ± 1.07	0.053 ± 0.021
PEC 1:2	1.89 ± 0.41	0.036 ± 0.008
PEC 1:3	2.07 ± 0.70	0.040 ± 0.014

$$t^+_{\text{solution}} = t_{(K^+)} = 0.49.$$

obstacle to the passage of yeast. The second reason is the electrostatic interaction between PEC and the yeast. The zeta potential of *S. cerevisiae* in the region of pH 6.0, close to the pH of the prepared yeast solution, is approximately -19 mV .³⁸ Therefore, electrostatic attraction between the amino groups of CH and the microorganisms is possible. It seems that increasing the SPEC content in PECs contributes to improve the yeast retention. However, the higher content of SPET results in decreasing number of $-\text{NH}_3^+$ groups for yeast interaction. In order to elucidate the high retention of *Saccharomyces* by PEC 1:2 membrane, the membrane potential of the samples was investigated.

From the microfiltration results, it is important to elucidate whether the PECs deposited onto the membrane surface can act as fixed charges. Since the presence of fixed charges is associated with the membrane permselectivity, the membrane potential and cation transport number (t^+) were measured.³⁰ Taking into

**Figure 11.** Relationship between *Saccharomyces* retention and normalized cation transport number as a function of SPET content.

account the t^+ of the cations in solution, the relation $\frac{t^+_{\text{polymer}}}{t^+_{\text{solution}}}$ can be used to predict the nature of the fixed charges in membrane as follows: (1) if relation = 1, there is no fixed charges in membrane; (2) relation >1 indicates negative fixed charges; and (3) relation <1 indicates positive fixed charges.³⁰ Table V presents the membrane potential and the t^+ obtained for PC-PECs membranes.

All modified membranes present $t^+_{\text{polymer}}/t^+_{\text{solution}} < 1$, indicating that these systems clearly possess fixed charges. Figure 11 shows that the yeast retention by the membranes is associated with $t^+_{\text{polymer}}/t^+_{\text{solution}}$. As previously discussed in WVT section, the tendency of the PECs clogs the membrane pores is similar, independently of the SPET content. Therefore, the electrostatic interaction plays a role more evident than the clog effect caused by the PECs into the membrane pores.

Consequently, it is possible to increase the yeast microfiltration performance of PC membranes using an easy and simple method of PEC deposition.

CONCLUSIONS

PELs complexes of chitosan and SPET can be obtained by an easy and rapid methodology. These particles have positive zeta potential values ranging from 28 to 40 mV, resulting in stable complexes. The thermogravimetric analysis indicated that the PELs complexes have good thermal stability thanks to the strong electrostatic attraction between the PELs. It has also been observed that the PELs complexes interact with polycarbonate membranes resulting in a stable surface deposition of the complexes. The PECs modify significantly the water affinity of the membranes resulting in an increasing in the water vapor flux. SPET content can control the number of cationic groups of the PECs. The tunable cationic nature of the obtained PECs contributes to increase the interaction with *S. cerevisiae*. Finally, the presence of the tunable PECs into polycarbonate membranes was able to produce a polymeric membrane with superior *S. cerevisiae* microfiltration performance.

ACKNOWLEDGMENTS

The authors thank CNPq for providing the financial support to this project. We also thank Ricardo Henrique Gonçalves for assistance with SEM and Darlan Gonçalves Nakayama for helping on the counting of microorganisms.

REFERENCES

- Du, J.; Sun, R.; Zhang, S.; Zhang, L.-F.; Xiong, C.-D.; Peng, Y.-X. *Biopolymers*. **2005**, *78*, 1.
- Cerchiara, T.; Abruzzo, A.; Parolin, C.; Vitali, B.; Bigucci, F.; Gallucci, M. C.; Nicoletta, F. P.; Luppi, B. *Carbohydr. Polym.* **2016**, *143*, 124.
- Ji, F.; Li, J.; Qin, Z.; Yang, B.; Zhang, E.; Dong, D.; Wang, J.; Wen, Y.; Tian, L.; Yao, F. *Carbohydr. Polym.* **2017**, *177*, 86.
- Mocchiutti, P.; Schnell, C. N.; Rossi, G. D.; Peresin, M. S.; Zanuttini, M. A.; Galván, M. V. *Carbohydr. Polym.* **2016**, *150*, 89.
- Kolman, K.; Nechyporchuk, O.; Persson, M.; Holmberg, K.; Bordes, R. *Colloids Surf. A Physicochem. Eng. Asp.* **2017**, *532*, 420.
- Yu, L.; Liu, X.; Yuan, W.; Brown, L. J.; Wang, D. *Langmuir*. **2015**, *31*, 6351.
- Coimbra, P.; Alves, P.; Valente, T. A. M.; Santos, R.; Correia, I. J.; Ferreira, P. *Int. J. Biol. Macromol.* **2011**, *49*, 573.
- Xu, C.; Xue, S.; Wang, P.; Wu, C.; Wu, Y. *Sep. Purif. Technol.* **2017**, *172*, 140.
- Ye, C.-C.; Zhao, F.-Y.; Wu, J.-K.; Weng, X.-D.; Zheng, P.-Y.; Mi, Y.-F.; An, Q.-F.; Gao, C.-J. *Chem. Eng. J.* **2017**, *307*, 526.
- Khulbe, K. C.; Feng, C.; Matsuura, T. *J. Appl. Polym. Sci.* **2010**, *115*, 855.
- Wang, H.; Wang, W.; Wang, L.; Zhao, B.; Zhang, Z.; Xia, X.; Yang, H.; Xue, Y.; Chang, N. *Chem. Eng. J.* **2018**, *334*, 2068.
- Ruan, H.; Zheng, Z.; Pan, J.; Gao, C.; Van der Bruggen, B.; Shen, J. *J. Membr. Sci.* **2018**, *550*, 427.
- Zhang, W.; He, G.; Gao, P.; Chen, G. *Sep. Purif. Technol.* **2003**, *30*, 27.
- Wavhal, D. S.; Fisher, E. R. *J. Membr. Sci.* **2002**, *209*, 255.
- Yue, W.-W.; Li, H.-J.; Xiang, T.; Qin, H.; Sun, S.-D.; Zhao, C.-S. *J. Membr. Sci.* **2013**, *446*, 79.
- Galiano, F.; André Schmidt, S.; Ye, X.; Kumar, R.; Mancuso, R.; Curcio, E.; Gabriele, B.; Hoinkis, J.; Figoli, A. *Sep. Purif. Technol.* **2018**, *194*, 149.
- Maya, E. M.; Muñoz, D. M.; de la Campa, J. G.; de Abajo, J.; Lozano, Á. E. *Desalination*. **2006**, *199*, 188.
- Upadhyaya, L.; Qian, X.; Ranil Wickramasinghe, S. *Curr. Opin. Chem. Eng.* **2018**, *20*, 13.
- Zhao, Q.; Qian, J.-W.; An, Q.-F.; Yang, Q.; Zhang, P. *J. Membr. Sci.* **2008**, *320*, 8.
- Kulkarni, A. D.; Vanjari, Y. H.; Sancheti, K. H.; Patel, H. M.; Belgamwar, V. S.; Surana, S. J.; Pardeshi, C. V. *Artif. Cells, Nanomed. Biotechnol.* **2016**, *44*, 1615.
- Stopilha, R. T.; de Lima, C. R. M.; Pereira, M. R.; Fonseca, J. L. C. *Colloids Surf. A Physicochem. Eng. Asp.* **2016**, *489*, 27.
- Senra, T. D. A.; Khoukh, A.; Desbrières, J. *Carbohydr. Polym.* **2017**, *156*, 182.
- Rinaudo, M. *Prog. Polym. Sci.* **2006**, *31*, 603.
- Luo, Y.; Wang, Q. *Int. J. Biol. Macromol.* **2014**, *64*, 353.
- Wan Ngah, W. S.; Teong, L. C.; Hanafiah, M. A. K. M. *Carbohydr. Polym.* **2011**, *83*, 1446.
- Kulig, D.; Zimoch-Korzycka, A.; Jarmoluk, A. *Meat Sci.* **2017**, *123*, 219.
- Paranhos, C. M.; Dahmouche, K.; Zaioncz, S.; Soares, B. G.; Pessan, L. A. *J. Polym. Sci. Part B Polym. Phys.* **2008**, *46*, 1390.
- Paranhos, C. M.; Soares, B. G.; Machado, J. C.; Windmöller, D.; Pessan, L. A. *Eur. Polym. J.* **2007**, *43*, 4882.
- Rege, P. R.; Block, L. H. *Carbohydr. Res.* **1999**, *321*, 235.

30. Tanaka, Y. Preparation of ion exchange membranes. In *Ion Exchange Membranes*, Elsevier: Amsterdam, Netherlands, **2015**.
31. Canella, K. M. N. d. C.; Garcia, R. B. *Quim. Nova.* **2001**, *24*, 13.
32. dos Santos, J. E.; Soares, J. d. P.; Dockal, E. R.; Campana Filho, S. P.; Cavalheiro, É. T. G. *Polímeros.* **2003**, *13*, 242.
33. Vijayakumar, S.; Rajakumar, P. R. *Int. Lett. Chem. Phys. Astron.* **2013**, *4*, 58.
34. Wang, H.; Li, W.; Lu, Y.; Wang, Z. *J. Appl. Polym. Sci.* **1997**, *65*, 1445.
35. Wan, Y.; Creber, K. A.; Peppley, B.; Bui, V. T. *Polymer (Guildf).* **2003**, *44*, 1057.
36. Yin, J.; Dai, Z.; Yan, S.; Cao, T.; Ma, J.; Chen, X. *Polym. Int.* **2007**, *56*, 1122.
37. Ruvolo-Filho, A.; Murakami, M. M. *J. Macromol. Sci. Part B.* **1998**, *37*, 627.
38. Narong, P.; James, A. E. *Sep. Purif. Technol.* **2006**, *49*, 149.